Optimal Approximations of Coupling in Multidisciplinary Models

Citation: Baptista, Ricardo et al. "Optimal Approximations of Coupling in Multidisciplinary Models." AIAA journal, vol. 56, no. 6, 2018, pp. 2412-2428 © 2018 The Author(s)

As Published: 10.2514/1.J056888

Publisher: American Institute of Aeronautics and Astronautics (AIAA)

Persistent URL: https://hdl.handle.net/1721.1/126539

Version: Author's final manuscript: final author's manuscript post peer review, without publisher's formatting or copy editing

Optimal Approximations of Coupling in Multidisciplinary Models

Ricardo Baptista[*], Youssef Marzouk[†], Karen Willcox[‡]
Massachusetts Institute of Technology, Cambridge, MA
and Benjamin Peherstorfer[§]
University of Wisconsin-Madison, Madison, WI

Design of complex engineering systems requires coupled analyses of the multiple disciplines affecting system performance. The coupling among disciplines typically contributes significantly to the computational cost of analyzing the system, and can become particularly burdensome when coupled analyses are embedded within a design or optimization loop. In many cases, disciplines may be weakly coupled, so that some of the coupling or interaction terms can be neglected without significantly impacting the accuracy of the system output. However, typical practice derives such approximations in an ad hoc manner using expert opinion and domain experience. This paper proposes a new approach that formulates an optimization problem to find a model that optimally balances accuracy of the model outputs with the sparsity of the discipline couplings. An adaptive sequential Monte Carlo sampling-based technique is used to efficiently search the combinatorial model space of different discipline couplings. Finally, an algorithm for optimal model selection is presented and applied to identify the important discipline couplings in a fire detection satellite model and a turbine engine cycle analysis model.

Nomenclature

$\mathbf{f}$	Model output variables (QoI)
$\mathbf{x}$	Model input variables
$\mathbf{y}$	Model state variables
$\mathcal{F}$	Function for output variables
$\mathcal{R}_i$	Residual function of discipline i
$\pi_{\mathbf{f}}$	Probability density of outputs
$\pi_{\mathbf{x}}$	Probability density of inputs
m	Number of input variables
n	Number of state variables
p	Number of output variables
Λ	Vector of tuning parameters
λ	Tuning parameter in discrete optimization
$\mathcal{M}$	Model space
$\mathcal{P}(M)$	Function to count removed couplings
$\mathcal{S}_k$	Input state variables to discipline k
d	Number of discipline couplings
D_{KL}	Kullback-Leibler divergence
K	Number of disciplines
M	Discipline couplings in the decoupled model
M_0	Discipline couplings in the reference model
$\mathbf{y}(\mu_{\mathbf{x}})$	First-order mean of state variables
$\mu_{\mathbf{x}}$	Mean of input variables
$\mu_{\tilde{\mathbf{f}}}$	Mean of linearized model output
$\Sigma_{\tilde{\mathbf{f}}}$	Covariance of linearized model output
$\tilde{\mathbf{f}}$	Linear approximation of model outputs
δ	Threshold for minimum sample diversity
$\rho(t)$	Tempering parameter at step t
ζ_t	Particle diversity at step t
L	Number of particles in SMC
$P_t(M)$	Probability of model M at step t
$w_t^{(l)}$	Weight of model l at step t
$\Delta t_{eclipse}$	Satellite: Eclipse period
Δt_{orbit}	Satellite: Orbit period
τ_{tot}	Satellite: Total torque
θ_{slew}	Satellite: Maximum slewing angle
A_{sa}	Satellite: Area of the solar array
C_d	Satellite: Drag coefficient

[*]Graduate Student, Center for Computational Engineering, rsb@mit.edu, AIAA Student Member
[†]Associate Professor, Department of Aeronautics and Astronautics, ymarz@mit.edu, AIAA Senior Member
[‡]Professor, Department of Aeronautics and Astronautics, kwillcox@mit.edu, AIAA Associate Fellow
[§]Assistant Professor, Department of Mechanical Engineering, peherstorfer@wisc.edu

F_s	Satellite: Average solar flux
H	Satellite: Altitude
H	Satellite: Deviation of moment axis
I	Satellite: Moment of inertia
L_a	Satellite: Aerodynamic torque moment arm
L_{sp}	Satellite: Radiation torque moment arm
P_{ACS}	Satellite: Power of attitude control system
P_{other}	Satellite: Power other than P_{ACS}
P_{tot}	Satellite: Total power
q	Satellite: Reflectance factor
R_D	Satellite: Residual dipole of spacecraft
v	Satellite: Satellite velocity
BPR	Turbine: Bypass ratio
CPR	Turbine: Compressor pressure ratio
F_n	Turbine: Net thrust
FPR	Turbine: Fan pressure ratio
OPR	Turbine: Overall pressure ratio
T_4	Turbine: Engine burner temperature
$TSFC$	Turbine: Thrust-specific fuel consumption
W	Turbine: Mass-flow rate

I. Introduction

Multidisciplinary analysis and optimization (MDAO) couples multiple computational models to represent complex interactions in the design of engineering systems. With the increasing number of disciplines and improved fidelity in multidisciplinary models, the coupling among disciplines can contribute significantly to the computational cost of analyzing these systems. This coupling may include both one-directional (feed-forward) coupling, and bi-directional (feedback) coupling that requires iterative numerical methods to compute a model solution. The coupled MDAO problem may be formulated in a variety of different ways,[1] and various MDAO architectures have been developed to manage discipline coupling for large-scale problems (see Ref. 2 for an overview). Monolithic architectures solve the system using a single optimization problem, while distributed approaches partition the model into subproblems, each involving a smaller number of variables.[3–7] Typical practice derives these discipline couplings using expert opinion and domain experience. Given the significant impact of couplings on the computational tractability of evaluating a model, it is of interest to systematically identify *which* disciplines should be coupled in a model and where couplings may be neglected. This paper addresses this open challenge to yield *optimal approximations* to coupling in multidisciplinary systems.

The application of MDAO originated in structural optimization and aircraft wing design.[8,9] It has since been extended to many different engineering systems, such as the design of complete aircraft configurations,[10,11] internal combustion engines,[12] wind turbines,[13] and spacecraft.[14] Multidisciplinary models of such systems often demonstrate varying degrees of coupling. Couplings can be categorized as being "strong" or "weak" based on the response of a discipline output to a change in a coupling variable.[15] As a result, for certain quantities of interest (QoI) in a model, neglecting weak interactions negligibly impacts the accuracy of the system outputs. Simultaneously, decoupling the disciplines reduces the number of feedback loops and presents a substantial computational savings when using the model for design optimization and/or uncertainty propagation. Therefore, an important challenge in the field of MDAO has been to identify the decoupled model that best trades the sparsity of the discipline couplings with the accuracy of the model in representing the engineering system. One approach to do this uses weighted design structure matrices to decompose the model and rearrange the disciplines to minimize feedback cycles. This method estimates the strength of couplings based on the discipline connectivity[16] or the sensitivity of model outputs to the coupling at each iteration of a multidisciplinary optimization process.[17] However, existing methods leave open the question of identifying which discipline couplings are most important in a model for characterizing system outputs over a range of input variables.

In this work we identify an optimal approximation to coupling in the context of multidisciplinary models under uncertainty. Using these models for optimization or uncertainty quantification is challenging as a result of the coupling between disciplines. Nevertheless, by taking into account the probabilistic information in the states of the system, we quantify the effect of neglecting each discipline coupling by measuring the information loss in the uncertainty of the model outputs. Combining this objective with a penalty term to promote sparsity in the number of couplings, we formulate a combinatorial optimization problem to explore the space of possible discipline couplings and find an optimal approximation to the multidisciplinary model.

For a model with K disciplines, there are $d = K^2 - K$ possible discipline couplings and the number of decoupled models grows exponentially as 2^d. As a result, comparing all possible decoupled models by enumeration is computationally intractable for large-scale systems. Instead, it is necessary to pursue alternative

approaches to search for the optimal discipline coupling. We leverage recent advances in adaptive sequential Monte Carlo (SMC) algorithms[18,19] to search efficiently over this model space.

The remainder of this paper is organized as follows. Sections II and III introduce the mathematical formulation and methodology to search efficiently for an optimal approximation to the coupling of a multidisciplinary model. Section IV presents results for two engineering systems: a fire detection satellite and a turbine engine cycle analysis model. Finally Section V concludes the paper and presents future research directions.

II. Background and Problem Formulation

This section introduces the notation and background for multidisciplinary model analysis in Sections II.A and II.B, and presents the problem formulation for model coupling approximations in Section II.C.

II.A. Multidisciplinary Models

Numerical multidisciplinary models consist of a set of equations that capture the relationships between input and output variables, mediated by the internal state variables of each discipline. While input variables are independent and defined externally by a user, output variables are quantities of interest (QoI) that depend on the input variables and the state variables of the model.

In this paper, $\mathbf{x} = [x_1, \ldots, x_m]^T \in \mathcal{X} \subseteq \mathbb{R}^m$ is a vector of m input variables, $\mathbf{y} = [y_1, \ldots, y_n]^T \in \mathcal{Y} \subseteq \mathbb{R}^n$ is a vector representing the n state variables, and $\mathbf{f} = [f_1, \ldots, f_p]^T \in \mathbb{R}^p$ is a vector of p output variables. Each state variable in the model, y_i, is defined implicitly by a governing residual equation

$$\mathcal{R}_i(\mathbf{x}, \mathbf{y}) = 0, \tag{1}$$

where in most generality the function $\mathcal{R}_i$ depends on all input and state variables, and consists of algebraic equations, PDEs, and/or other operations. The function $\mathcal{F}\colon \mathcal{X} \times \mathcal{Y} \to \mathbb{R}^p$ computes the output variables explicitly as

$$\mathbf{f} = \mathcal{F}(\mathbf{x}, \mathbf{y}). \tag{2}$$

Letting $\mathcal{R} = [\mathcal{R}_1, \ldots, \mathcal{R}_n]^T$, a numerical model is represented by the coupled system of equations, $\mathcal{R}(\mathbf{x}, \mathbf{y}) = \mathbf{0}$, where $\mathcal{R}\colon \mathcal{X} \to \mathcal{Y}$. In a multidisciplinary problem, the n residual equations (1) are partitioned into disjoint groups representing each particular engineering discipline or subsystem of the model. These disciplines also define a partitioning of the vector of state variables, $\mathbf{y}$. This vector consists of state variables that are local to each discipline, and coupling variables that affect the residual equations in different disciplines. A graphical representation of these coupling variables in a model with two disciplines is given in Figure 1. We note that in the displayed model, only one residual function and state variable is associated with each discipline.

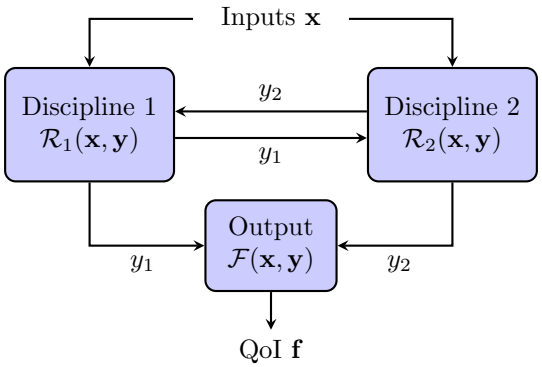

Figure 1. Graphical representation of a generic multidisciplinary model

The dependence of the residual equations on coupling variables from other disciplines defines the overall discipline coupling in the model. This coupling can include one-directional (feed-forward) coupling, or bi-directional (feedback) coupling between any two disciplines. For instance, the dependence of both disciplines on the same subset of state variables in Figure 1 results in feedback coupling in this model. Solving these systems of feedback coupled residual equations requires using an iterative numerical method to determine the states and corresponding output variables. Common iterative methods include fixed point iteration or more sophisticated algorithms for solving nonlinear equations, such as Newton-based approaches.

II.B. Uncertainty in Multidisciplinary Models

In many multidisciplinary models, the input variables are not known exactly. As an example, when analyzing a rocket during launch, it is common to consider wind gusts as a source of uncertainty in the multidisciplinary model.[20] In such cases, the input variables, $\mathbf{x}$, are represented as random variables endowed with a probability density function $\pi_{\mathbf{x}}$.

With uncertain inputs, the output variables of the model, $\mathbf{f}$, are also random variables endowed with a probability density function, $\pi_{\mathbf{f}}$. Forward uncertainty quantification (UQ) propagates the input uncertainty through the coupled model to characterize the uncertainty in the output variables. For engineering applications, this typically includes determining the mean and variance of the output variables, although sometimes other properties of the output distribution are also of interest.

For linear residual and output equations, the mean and variance in the output variables can be quantified analytically in terms of the model equations and the mean and variance of the inputs. However, for general nonlinear equations, forward UQ is more challenging and is commonly performed with various probabilistic techniques such as simulation-based methods, local model expansions, functional approximations, etc.[21]

One traditional and robust algorithm for quantifying uncertainty is based on Monte Carlo simulation. This sampling-based method draws N realizations of the input variables from $\pi_{\mathbf{x}}$. Each realization defines a sample, where $\mathbf{x}^{(j)}$ denotes the j-th sample of $\mathbf{x}$ for $j = 1, \ldots, N$. For each sample, the algorithm solves the coupled residual equations, $\mathcal{R}(\mathbf{x}^{(j)}, \mathbf{y}^{(j)}) = \mathbf{0}$ to determine the state $\mathbf{y}^{(j)}$, and evaluates $\mathbf{f} = \mathcal{F}(\mathbf{x}^{(j)}, \mathbf{y}^{(j)})$ to determine the output variables $\mathbf{f}^{(j)}$ for sample j. These samples are used to estimate the mean, variance, or other statistics of the probability distribution for the output variables, $\pi_{\mathbf{f}}$.

However, it is well known that the variance in Monte Carlo estimators converges at a rate of $\frac{1}{\sqrt{N}}$ with an increasing number of samples, N.[21] As a result, for expensive simulations under limited computational resources, this motivates the use of alternative techniques that reduce the computational cost of solving the multidisciplinary model. One approach for efficiently propagating uncertainty in multidisciplinary systems is a decomposition-based method that combines Monte Carlo sampling of each discipline or domain with importance sampling to analyze the uncertainty in feed-forward systems.[22] For multidisciplinary systems with feedback, recent methods include a likelihood-based approach to decouple feedback loops and reduce the model to a feed-forward system,[23] dimension reduction techniques to represent certain coupling variables with spectral expansions that depend on a small number of uncertain parameters,[24–26] and the use of adaptive surrogate models for individual disciplines[27] or to approximate the coupling variables and reduce the number of model evaluations.[28]

In this work we focus on approximate coupling as a way to reduce the computational cost of finding a solution to the multidisciplinary model. We note that this could also be combined with existing techniques to accelerate forward uncertainty quantification and model coupled analyses.

II.C. Model Coupling Approximation

Our approach of approximate coupling is to minimize the number of coupling variables between disciplines. In practice, many disciplines are often weakly coupled and the residual equations in each discipline are most sensitive to only a subset of the coupling variables.[15] Therefore, the coupling variables that have a minor effect on the state variables computed by each discipline can be fixed to a nominal value, while incurring a small effect on the discipline output. Furthermore, by removing the dependence of a discipline on certain

coupling variables, we decouple the corresponding disciplines. Ultimately, this reduction in discipline coupling minimizes the number of iterations required to find a converged solution to the system.

In a multidisciplinary model with K disciplines, we define $\mathcal{S}_k \subseteq \{y_1, \ldots, y_n\}$ as the set of coupling variables that are arguments to the residual functions in the k-th discipline. The set of discipline couplings in each model is then given by $M = (\mathcal{S}_1, \ldots, \mathcal{S}_K)$, where the total number of discipline couplings is $d(M) = \sum_{k=1}^{K} |\mathcal{S}_k|$. For a multidisciplinary model with a set of defined discipline couplings, our goal in this work is to find the coupling variables (i.e. $y_i \in S_k$ for all k) that have a small effect on the overall model output. Each of these variables are then fixed to a nominal value, such as their mean value, and removed from S_k, thereby decoupling the two disciplines.

The operation of replacing the dependence of residual equation, $\mathcal{R}_2$, on the coupling variable, y_1, with the fixed constant input, $\overline{y_1}$, is seen graphically in Figures 2 and 3. By decoupling discipline 1 from 2, the original feedback coupled multidisciplinary model is converted into a feed-forward model. In this case, instead of having to iteratively solve the coupled residual equations to find $\mathbf{y}$, the state variables can be more cheaply determined by solving the one-way coupled model.

For the remainder of this paper, we denote the set of discipline couplings in our reference multidisciplinary model as M_0, and use M to represent a model that results from decoupling two or more disciplines.

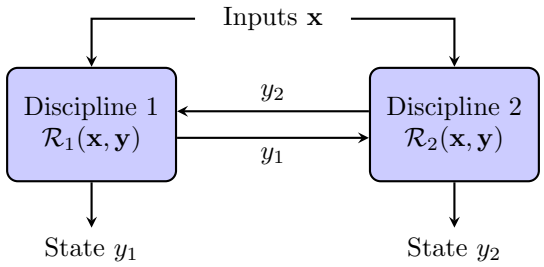

Figure 2. Feedback coupled two discipline model, M_0

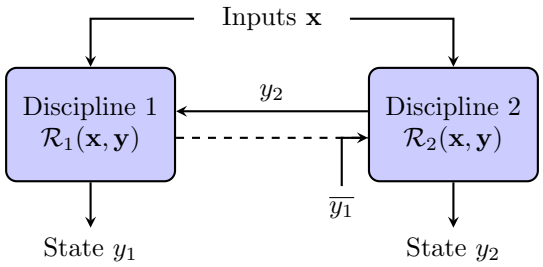

Figure 3. One-way coupled two discipline model, M

In the context of forward UQ, the error introduced by decoupling the model disciplines is defined as the accuracy of the probability distribution for the output variables in model M. This accuracy is measured by the Kullback-Leibler (KL) divergence between the probability distribution of the output variables in the decoupled model, $\pi_{\mathbf{f}_M}$, and the distribution of the outputs in the reference model, $\pi_{\mathbf{f}_{M_0}}$. The KL divergence is denoted by $D_{KL}(\pi_{\mathbf{f}_{M_0}} || \pi_{\mathbf{f}_M})$ and is non-zero when the distributions for the output variables of the two models are not equal almost everywhere. As a result, the KL divergence provides an indication of the information lost when using $\pi_{\mathbf{f}_M}$ to approximate the distribution of the output variables with the discipline couplings, M. The reader is referred to Ref. 29 for more properties on the KL divergence.

Therefore, to reduce the computational cost of solving the multidisciplinary model, we search for the maximum number of disciplines that can be decoupled while minimizing the KL divergence. These competing objectives are used to formulate a combinatorial optimization problem to find an optimal subset of discipline couplings by exploring the space of possible decoupled models, which we denote by $\mathcal{M}$. To represent the two parts of the objective function, we use the KL divergence as a measure for the accuracy of the output variable distributions in both models, and use the function $\mathcal{P}\colon \mathcal{M} \to \mathbb{N}$ to represent the sparsity of the model couplings. In this work, $\mathcal{P}(M) = d(M_0) - d(M)$, i.e., the function counts the number of removed discipline couplings for each possible model, M. Finally, these parts are combined in the objective function by using a tuning parameter, λ, that controls the relative importance given to accuracy vs. sparsity.

With this objective, the optimally decoupled model, which we denote by $M^*(\lambda)$, is found by solving the optimization problem

$$M^*(\lambda) = \underset{M \in \mathcal{M}}{\arg\min}\ D_{KL}(\pi_{\mathbf{f}_{M_0}} || \pi_{\mathbf{f}_M}) - \lambda \mathcal{P}(M). \tag{3}$$

We note that other metrics can also be used for the sparsity penalty, $\mathcal{P}(M)$, in the optimization problem. For example, by using additional knowledge about the contribution of each discipline coupling to the total cost

of running the model, we can assign a different weight to each coupling that favors removing computationally expensive discipline couplings.

For a model with K disciplines and d discipline couplings, d can grow as $d = K^2 - K$ for a fully coupled model. With each coupling being either active or inactive, the total size of the space of possible models, $\mathcal{M}$, grows exponentially with cardinality $|\mathcal{M}| = 2^d$. As a result, it is not feasible to compare models with many disciplines by enumeration. Instead, the next section discusses an approach based on a particle method to efficiently explore the high-dimensional model space and find the optimal model, M^*.

III. Approximate Coupling via Optimization

This section introduces the use of model linearizations for estimating the KL divergence in Section III.A, and addresses the combinatorial optimization problem that was posed in equation 3 in Sections III.B and III.C.

III.A. Model Linearization

The first term in the objective function (3) represents the accuracy of the output distributions for a possible model M relative to the reference model, M_0. One approach to evaluate this term is to generate samples for the output variables and to use the samples to approximate the KL divergence with density estimation techniques.[30] However, for large-scale multidisciplinary models, it is not feasible to generate many samples from multiple models via Monte Carlo simulations by repeatedly solving the coupled equations.

As a result, we propose to use a linear approximation for each model to efficiently estimate the KL divergence of the probability distributions for the output variables. The linearization of a multidisciplinary model is given by the first order Taylor series approximation of the model outputs given in equation 2. This linearization is found by evaluating the partial derivatives of the function $\mathcal{F}$ with respect to input and state variables, which are denoted by $\partial_{\mathbf{x}}\mathcal{F}$ and $\partial_{\mathbf{y}}\mathcal{F}$, respectively. Both of these derivatives are evaluated at a specific linearization point for the input and state variables.

One natural linearization point is based on the mean of the state variables, $\mathbf{y}$. However, finding the mean requires characterizing the distribution for these variables *a-priori*. Instead, an approximation commonly employed in the literature[23] is to linearize the models around the state variables corresponding to the mean values of the input variables. The mean value of $\mathbf{x}$ is denoted by $\mu_{\mathbf{x}} = \mathbb{E}[\mathbf{x}]$ where $\mathbb{E}$ is the expectation operator with respect to the probability distribution $\pi_{\mathbf{x}}$. The state variables corresponding to $\mu_{\mathbf{x}}$ satisfy the residual equations, $\mathcal{R}(\mu_{\mathbf{x}}, \mathbf{y}(\mu_{\mathbf{x}})) = \mathbf{0}$, and these states are referred to as a first-order mean for $\mathbf{y}$.[31]

Using the Taylor series expansion about the first-order mean, the linearized approximation of the output variables is given by

$$\mathbf{f} = \mathcal{F}(\mathbf{x}, \mathbf{y}) \approx \mathcal{F}(\mu_{\mathbf{x}}, \mathbf{y}(\mu_{\mathbf{x}})) + \partial_{\mathbf{x}}\mathcal{F}|_{\mu_{\mathbf{x}}, \mathbf{y}(\mu_{\mathbf{x}})} (\mathbf{x} - \mu_{\mathbf{x}}) + \partial_{\mathbf{y}}\mathcal{F}|_{\mu_{\mathbf{x}}, \mathbf{y}(\mu_{\mathbf{x}})} (\mathbf{y} - \mathbf{y}(\mu_{\mathbf{x}})). \tag{4}$$

Similarly, the linearized approximation of the coupled residual equations for the model is given by

$$\mathcal{R}(\mathbf{x}, \mathbf{y}) \approx \mathcal{R}(\mu_{\mathbf{x}}, \mathbf{y}(\mu_{\mathbf{x}})) + \partial_{\mathbf{x}}\mathcal{R}|_{\mu_{\mathbf{x}}, \mathbf{y}(\mu_{\mathbf{x}})} (\mathbf{x} - \mu_{\mathbf{x}}) + \partial_{\mathbf{y}}\mathcal{R}|_{\mu_{\mathbf{x}}, \mathbf{y}(\mu_{\mathbf{x}})} (\mathbf{y} - \mathbf{y}(\mu_{\mathbf{x}})), \tag{5}$$

where $\partial_{\mathbf{x}}\mathcal{R}$ and $\partial_{\mathbf{y}}\mathcal{R}$ denote the partial derivatives of the residuals with respect to the input and state variables, respectively. Rearranging the approximation in equation 5 for the state variables, and noting that $\mathcal{R}(\mu_{\mathbf{x}}, \mathbf{y}(\mu_{\mathbf{x}})) = \mathbf{0}$, a linear approximation to the state variables with respect to $\mathbf{x}$ is given by

$$\mathbf{y} = \mathbf{y}(\mu_{\mathbf{x}}) - (\partial_{\mathbf{y}}\mathcal{R}|_{\mu_{\mathbf{x}}, \mathbf{y}(\mu_{\mathbf{x}})})^{-1} \partial_{\mathbf{x}}\mathcal{R}|_{\mu_{\mathbf{x}}, \mathbf{y}(\mu_{\mathbf{x}})} (\mathbf{x} - \mu_{\mathbf{x}}). \tag{6}$$

Here we note that the matrix of partial derivatives, $(\partial_{\mathbf{y}}\mathcal{R})^{-1}\partial_{\mathbf{x}}\mathcal{R}$ in equation 6, contains the sensitivity of the state variables to perturbations in the inputs. These sensitivities to the input variables are often computed as part of an adjoint analysis for single or multiple discipline models.[32,33] Furthermore, the sensitivities

are typically found without assembling and inverting the full matrix of partial derivatives of the residual equations with respect to the state variables. Instead, the values in the matrix are determined by solving a linear system with an iterative numerical method.[2]

Substituting the linearization for the state variables in equation 4, a linear approximation to the sensitivity of the output QoIs in the multidisciplinary model with respect to the input parameters, $\mathbf{x}$, is given by

$$\begin{aligned}\mathbf{f} \approx \tilde{\mathbf{f}}(\mathbf{x}) &= \mathcal{F}(\mu_{\mathbf{x}}, \mathbf{y}(\mu_{\mathbf{x}})) + \left[\partial_{\mathbf{x}}\mathcal{F}|_{\mu_{\mathbf{x}},\mathbf{y}(\mu_{\mathbf{x}})} - \partial_{\mathbf{y}}\mathcal{F}|_{\mu_{\mathbf{x}},\mathbf{y}(\mu_{\mathbf{x}})} \left(\partial_{\mathbf{y}}\mathcal{R}|_{\mu_{\mathbf{x}},\mathbf{y}(\mu_{\mathbf{x}})}\right)^{-1} \partial_{\mathbf{x}}\mathcal{R}|_{\mu_{\mathbf{x}},\mathbf{y}(\mu_{\mathbf{x}})}\right](\mathbf{x} - \mu_{\mathbf{x}}) \\ &= \mathcal{F}(\mu_{\mathbf{x}}, \mathbf{y}(\mu_{\mathbf{x}})) + \left.\frac{d\mathcal{F}}{d\mathbf{x}}\right|_{\mu_{\mathbf{x}},\mathbf{y}(\mu_{\mathbf{x}})} (\mathbf{x} - \mu_{\mathbf{x}}),\end{aligned} \tag{7}$$

where $\tilde{\mathbf{f}}(\mathbf{x})$ represents the linear approximation to the output QoI and $\frac{d\mathcal{F}}{dx}$ denotes the matrix of total derivatives of $\mathcal{F}$ with respect to the input variables. With this linear relationship in the inputs, $\mathbf{x}$, the mean and variance of the linearized outputs are propagated analytically from the mean and variance of the input variables. In particular, if the input variables are normally distributed with covariance matrix, $\Sigma_{\mathbf{x}}$, the linearized output variables are also normally distributed with mean, $\mu_{\tilde{\mathbf{f}}} = \mathbb{E}[\tilde{\mathbf{f}}]$, and covariance, $\Sigma_{\tilde{\mathbf{f}}} = \mathbb{E}[(\tilde{\mathbf{f}} - \mu_{\tilde{\mathbf{f}}})(\tilde{\mathbf{f}} - \mu_{\tilde{\mathbf{f}}})^T]$, where

$$\mu_{\tilde{\mathbf{f}}} = \mathcal{F}(\mu_{\mathbf{x}}, \mathbf{y}(\mu_{\mathbf{x}})), \tag{8}$$

$$\Sigma_{\tilde{\mathbf{f}}} = \left[\left.\frac{d\mathcal{F}}{d\mathbf{x}}\right|_{\mu_{\mathbf{x}},\mathbf{y}(\mu_{\mathbf{x}})}\right] \Sigma_x \left[\left.\frac{d\mathcal{F}}{d\mathbf{x}}\right|_{\mu_{\mathbf{x}},\mathbf{y}(\mu_{\mathbf{x}})}\right]^T. \tag{9}$$

To compute the KL divergence for the output variables of each decoupled model, $M \in \mathcal{M}$, relative to the reference model, M_0, we compute the mean and covariance of the linearized model outputs using 8 and 9. The mean and covariance for the linearized output variables of model M_0 are denoted by $\mu_{\tilde{\mathbf{f}}_{M_0}}$ and $\Sigma_{\tilde{\mathbf{f}}_{M_0}}$, respectively. Similarly, the mean and covariance for the decoupled model M are denoted by $\mu_{\tilde{\mathbf{f}}_M}$ and $\Sigma_{\tilde{\mathbf{f}}_M}$, respectively. Using the closed form expression for the KL divergence between two Gaussian distributions, we estimate the KL divergence between the probability distributions for the outputs of models M_0 and M with the equation

$$D_{KL}(\pi_{\tilde{\mathbf{f}}_{M_0}} || \pi_{\tilde{\mathbf{f}}_M}) = \frac{1}{2}\left\{\mathrm{Tr}(\Sigma_{\tilde{\mathbf{f}}_M}^{-1}\Sigma_{\tilde{\mathbf{f}}_{M_0}}) + (\mu_{\tilde{\mathbf{f}}_M} - \mu_{\tilde{\mathbf{f}}_{M_0}})^T\Sigma_{\tilde{\mathbf{f}}_M}^{-1}(\mu_{\tilde{\mathbf{f}}_M} - \mu_{\tilde{\mathbf{f}}_{M_0}}) - p + \ln\left(\frac{|\Sigma_{\tilde{\mathbf{f}}_M}|}{|\Sigma_{\tilde{\mathbf{f}}_{M_0}}|}\right)\right\}, \tag{10}$$

where $\mathrm{Tr}(\cdot)$ denotes the matrix trace operator, and $\ln(|\cdot|)$ is the log-determinant of a matrix. We note that the derivatives in expression 7 are typically available when computing system outputs or performing design optimization. This leads to a small incremental cost for evaluating the KL divergence in equation 10. Furthermore, while higher-order expansions of the residual functions may provide improved accuracy approximations in highly nonlinear regimes for the outputs,[3,4] the probability distributions resulting from these higher order expansions to the output variables cannot be compared using an analytic expression. Instead, these approximations require generating samples from the distribution and using density estimation techniques to estimate the KL divergence.

It is also important to note that each decoupled model, $M \in \mathcal{M}$, results in a different first-order mean for the state variables. As a result, to compute the mean and covariance for the output variables, it is necessary to solve the nonlinear residual equations once for each M at the mean input variables. The resulting first-order mean of $\mathbf{y}$ is then used as the linearization point to evaluate the partial derivatives of the residual and output functions in the model linearization. Finally, we also note that the effect of decoupling disciplines is also seen with the additional sparsity in the $\partial_{\mathbf{y}}\mathcal{R}$ matrix when the corresponding residual equations no longer depend on certain coupling variables from other disciplines.

However, finding the optimal solution to the combinatorial optimization problem posed in equation 3 still requires a method to explore the potentially multi-modal model space without enumerating all models. As a result, the following section will address this question using a particle method.

III.B. Sequential Monte Carlo

To find the optimal decoupled model that best balances the accuracy and sparsity of the approximate model coupling, we solve the combinatorial optimization problem in equation 3 that was proposed in Section II.C. With the increase in the cardinality of the model space, $\mathcal{M}$, the complexity of finding an optimal solution to this problem increases exponentially. As a result, common algorithms for combinatorial optimization problems find approximate solutions by using local neighborhood searches, depth-first branch and bound searches, or randomized methods such as simulated annealing and genetic algorithms. For a comparison of these methods, the reader is referred to Ref. 35.

To effectively explore the model space, there is growing numerical evidence that global particle methods based on sequential Monte Carlo (SMC), which track a population of possible solutions, are robust and can often outperform heuristics and local search methods for discrete optimization problems.[36,37] This is particularly evident in strongly multi-modal objective functions where local search methods can become trapped in certain modes of the model space. As a result, in this paper we chose to use SMC to perform the combinatorial optimization.

Although SMC is described in more detail below and summarized in Algorithm 1, the main steps are:

1. Generate a set of weighted particles representing possible decoupled models
2. Update the weights based on the value of the objective function
3. Propose new particles to explore the space while converging to the optimal solution
4. Repeat steps **2-3**

To find the optimal solution using SMC, we first define a sequence of probability distributions on the model space, which we denote by $P_t \colon \mathcal{M} \to [0,1]$ for each index $t \in \mathbb{N}$. These distributions progress from a distribution that is easy to sample from, such as the uniform weighting over the set of all possible decoupled models (i.e., $P_0(M) = \mathcal{U}(M)$), to the final distribution of interest that concentrates most mass over the models that minimize the objective function. To smoothly move towards the final target distribution, the goal of an efficient particle method is to learn the correlations and properties of the model space in order to find the global minimizers without enumerating all models.

Particle methods approximate the distribution at each step by a finite set of $L \in \mathbb{N}$ weighted particles that each represent a particular model. We denote particle l and step t of the algorithm by $M_t^{(l)}$ for $l = 1, \ldots, L$. Each of these particles is also associated with a weight that we denote by $w_t^{(l)}$. The collection of particles and weights at each step is given by $(\mathbf{M}_t, \mathbf{w}_t) = \{M_t^{(l)}, w_t^{(l)}\}_{l=1}^{L}$. While the weights are set to $1/L$ when initializing the system at $t = 0$, at each iteration of the algorithm the weights are updated based on the subsequent distributions using the ratio

$$u_{t+1}^{(l)} := w_t^{(l)} \frac{P_{t+1}(M_t^{(l)})}{P_t(M_t^{(l)})}, \tag{11}$$

followed by the normalization step, $w_{t+1}^{(l)} = u_{t+1}^{(l)} / \sum_l u_{t+1}^{(l)}$ for $l = 1, \ldots, L$. Here we note that it is sufficient to evaluate the models at the unnormalized versions of P_t and P_{t+1} given that the weight only requires the ratios of these probability mass functions. As described in a recent study by Shafer et al.,[37] one common and successful technique to construct these distributions over the model space is to use a tempered family. This family of distributions assigns to each decoupled model, $M \in \mathcal{M}$, the probability mass

$$P_t(M) \propto \exp(-\rho(t) h(M)), \tag{12}$$

where $h \colon \mathcal{M} \to \mathbb{R}_+$ is the value of the objective function for each model in the combinatorial optimization problem, and $\rho \colon \mathbb{N} \to \mathbb{R}_+$ is a monotonically increasing tempering parameter that depends on step t. For the combinatorial optimization problem posed in equation 3, the objective function is given by $h(M) = D_{KL}(\pi_{\tilde{\mathbf{f}}_{M_0}} || \pi_{\tilde{\mathbf{f}}_M}) - \lambda \mathcal{P}(M)$. Therefore, as t and $\rho(t)$ increase at each iteration, the tempered family concentrates more mass on the set of models that minimize the value for the objective function by assigning higher weights to these models. However, by just repeatedly re-weighing the initial set of particles

using equation 11, the weights will become uneven and eventually lead to particle degeneracy with a poor importance sampling approximation to each distribution.

As a result, the main ingredient that differentiates sequential Monte Carlo samplers from classical importance sampling is the series of alternating re-weighting and update steps that re-sample and move the particles in order to explore the space outside of the current set of models. By measuring a series of metrics including the effective sample size and the particle diversity, that are denoted by $ESS(\mathbf{w}_t)$ and $\zeta(\mathbf{M}_t, \mathbf{w}_t)$, respectively, SMC re-samples the particles from its current empirical distribution and moves them by using an adapted proposal distribution that samples new particles in the model space. This combination of steps ensures there is a smooth transition between all distributions, P_t, and they converge to the target based on an appropriate choice for the tempering parameter, $\rho(t)$.

Following the study in Ref. 37, we use systematic re-sampling to generate more samples corresponding to the particles with larger weights. Furthermore, we construct an independent proposal for the move steps that is adapted by using maximum likelihood estimation with the set of samples and weights at each iteration. As demonstrated in Ref. 18, this adaptive proposal results in faster exploration of the model space by drawing particles with a higher rate of acceptance.

The re-sample and move steps are repeated until the sample diversity drops below a threshold given by $\delta > 0$, indicating that most of the mass in $P_t(M)$ is concentrated on a few decoupled models. At the end, the algorithm returns the maximizer of the final distribution within this small set of particles as the optimally decoupled model. For the purposes of completeness, a summary of the algorithm to find the optimal model coupling is presented in Algorithm 1. Nevertheless, the reader is referred to Ref. 37 for more specific details on each function in the SMC algorithm for solving combinatorial optimization problems.

Algorithm 1: SMC for Optimal Model Coupling

Input: Model Objective Function: $h(M)$, Minimum Particle Diversity: δ, Number of Particles: L

Initialize counter: t $= 0$;
Sample models: $M_t^{(l)} \overset{iid}{\sim} \mathcal{U}(M)$ for $l = 1, \ldots, L$;
Initialize weights: $w_t^{(l)} = 1/L$ for $l = 1, \ldots, L$;
Compute particle diversity: $\zeta_t = \zeta(\mathbf{M}_t, \mathbf{w}_t)$;
while $\zeta_t > \delta$ **do**
    Update counter: $t \leftarrow t + 1$;
    Fit proposal: $q_t \leftarrow$ `Fit_Proposal`$(\mathbf{M}_t, \mathbf{w}_t)$;
    Re-sample: $\mathbf{M}_t \leftarrow$ `Re_sample`$(\mathbf{M}_t, \mathbf{w}_t)$;
    Move models: $\mathbf{M}_t \leftarrow$ `Move`$(q_t, \mathbf{M}_t, \mathbf{w}_t)$;
    Update $\rho(t)$ to maintain a minimum $ESS(\mathbf{w}_t)$;
    Update weights: $\mathbf{w}_t \leftarrow$ `Importance_Weights`$(h(M), \mathbf{M}_t, \mathbf{w}_t)$;
    Compute particle diversity: $\zeta_t = \zeta(\mathbf{M}_t, \mathbf{w}_t)$;
end
Return $M^* = \arg\min_{M \in \mathbf{M}_t} f(M)$, $f(M^*)$

In practice, the number of particles at each iteration of the SMC algorithm, L, and the minimum particle diversity, δ, are chosen relative to the cardinality of the model space. While the number of particles should be small enough to ensure that the model selection is computationally feasible, it should also be large enough to approximately represent the distributions, P_t. Furthermore, in all of our numerical examples we choose a minimum particle diversity of $\delta = 0.1L$ to terminate the algorithm and indicate that most probability mass is concentrated on a small number of unique particles.

III.C. Model Selection Procedure

Combining the sequential Monte Carlo algorithm presented above with the model linearizations for estimating the KL divergence, an optimally decoupled model, $M^*(\lambda)$, is determined for each value of λ in the objective

function. However, in an engineering setting, it is of interest to select the model coupling approximation based on accuracy requirements and the availability of computational resources.

To do so, we repeat the combinatorial optimization problem for different values of λ that are specified in the vector denoted by Λ. This provides a set of candidate models that balance accuracy and sparsity differently in the optimally decoupled model. While a heavier weight is placed on finding sparse models for larger values of λ, a heavier weight is placed on finding accurate models for smaller values of λ. As a result, by increasing λ, the optimal model trades-off accuracy in the distributions of the output variables relative to M_0 with having a smaller number of discipline couplings. By finding the optimal model for each value of λ using Algorithm 1, a user can select one of these models for their application by comparing the accuracy of each model to the computational cost of its sample evaluations. A summary of the complete algorithm for optimal model selection is presented in Algorithm 2.

Algorithm 2: Optimal Model Selection

Input: Reference multidisciplinary model: M_0, Input variable uncertainty: $\pi_{\mathbf{x}}$, Vector of objective function parameters: Λ, Model sparsity function: $\mathcal{P}(M)$

1 Linearize output variables of M_0 at mean of $\pi_{\mathbf{x}}$: $\tilde{\mathbf{f}}$;
2 Compute output uncertainty of $\tilde{\mathbf{f}}$: $\pi_{\tilde{\mathbf{f}}_{M_0}}$;
3 **for** $\lambda \in \Lambda$ **do**
4 Setup objective function: $h(M) = D_{KL}(\pi_{\tilde{\mathbf{f}}_{M_0}} || \pi_{\tilde{\mathbf{f}}_M}) - \lambda \mathcal{P}(M)$;
5 Determine $M^*(\lambda)$ using Algorithm 1;
6 **end**
7 Select optimal model by comparing the accuracy and sparsity of $M^*(\lambda)$ for each $\lambda \in \Lambda$;

IV. Numerical Results

In this section, we present results for applying the proposed model selection algorithm to two aerospace engineering examples. These are a three-discipline model of a satellite used to detect forest fires in Section IV.A that was presented in an uncertainty quantification context by Sankararaman et al.,[23] and a model for turbine engine cycle analysis in Section IV.B that was developed by Hearn et al.[38]

IV.A. Fire Detection Satellite Model

To analyze the performance of a fire detection satellite under uncertain operating conditions, we consider a simplified model that comprises three disciplines: orbit analysis, attitude control, and power analysis. As seen in Figure 4, the model features both feed-forward and feedback coupling variables to exchange information between the disciplines.

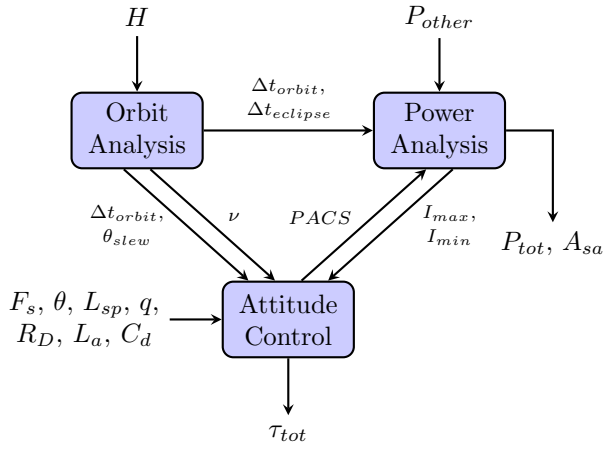

Figure 4. Fire detection satellite model from Ref. 23

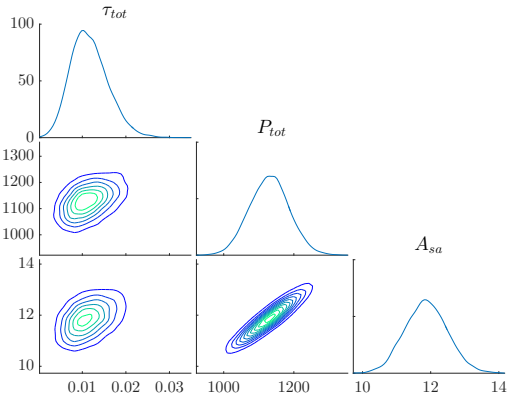

Figure 5. Joint distributions of the reference model

To represent the uncertain conditions, the model includes nine Gaussian random variables that are described by their mean and standard deviation parameters in Table 1. After propagating this input uncertainty through the disciplines, the seven state variables connecting the disciplines are also uncertain and are distributed with potentially non-Gaussian probability distributions. These state variables are: the orbit period (Δt_{orbit}), eclipse period ($\Delta t_{eclipse}$), satellite velocity (v), maximum slewing angle (θ_{slew}), the power of the attitude control system (P_{ACS}), and the moments of inertia (I_{max}, and I_{min}). In addition, the orbit period is an input to two disciplines (orbit analysis and attitude control) resulting in a total of $d = 8$ coupling variables for this satellite model as seen in Figure 4. These coupling variables are used to compute the three output QoIs: total torque (τ_{tot}), total power (P_{tot}), and the area of the solar array (A_{sa}). The joint probability distribution of these output variables, $\pi_{\mathbf{f}}$, is displayed in Figure 5.

Table 1. Random variable parameters in the satellite model from Ref. 23

Random Variable	Symbol	Mean	Standard Deviation
Altitude	H	18.0×10^6 m	1.0×10^6 m
Power other than attitude control	P_{other}	1.0×10^3 W	50.0 W
Average solar flux	F_s	1.4×10^3 W/m^2	20.0 W/m^2
Deviation of moment axis	θ	15.0°	1.0°
moment arm for radiation torque	L_{sp}	2.0 m	0.4 m
Reflectance factor	q	0.5	1.0
Residual dipole of spacecraft	R_D	5.0 Am^2	1.0 Am^2
Moment arm for aerodynamic torque	L_a	2.0 m	0.4 m
Drag coefficient	C_d	1.0	0.3

By defining the model displayed in Figure 4 as the reference model, M_0, our algorithm for optimal model selection considers decoupled models, M, that have a smaller number of discipline couplings by fixing a subset of the coupling variables of each discipline to their first-order mean value. In order to empirically validate the use of model linearizations to estimate the KL divergence of the decoupled models, we compare the Gaussian distribution for the linearized outputs of the reference model to the uncertainty in the output variables of the nonlinear coupled system based on 10^4 Monte Carlo samples. As seen in Figure 6, the joint empirical distribution for the output variables, $\pi_{\mathbf{f}}$, is closely approximated by the multivariate Gaussian distribution resulting from the linearized equations in expression 7.

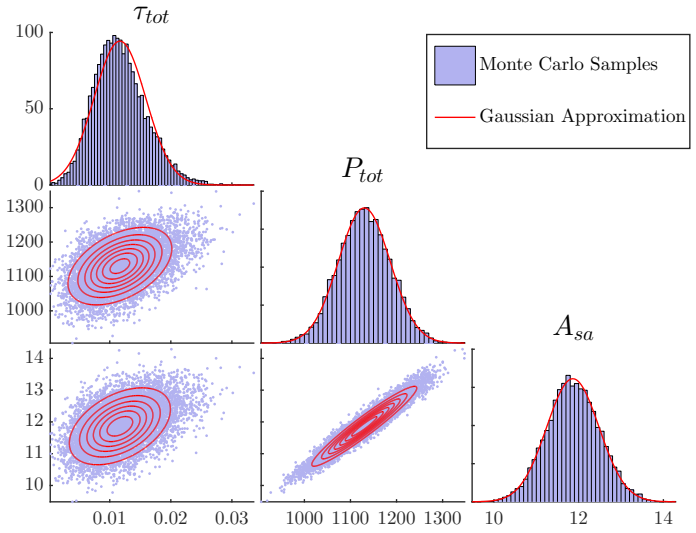

Figure 6. Comparison of Gaussian approximation and Monte Carlo samples

Using these linearizations for the output variables, the SMC algorithm explores the model space using $L = 100$ particles to determine the optimal decoupled model, $M^*(\lambda)$, that solves the combinatorial optimization problem posed in equation 3. For each value of λ, the algorithm identifies a subset of discipline couplings that best trade-off the accuracy of the output distributions, that is estimated by the $D_{KL}(\pi_{\tilde{\mathbf{f}}_{M_0}} || \pi_{\tilde{\mathbf{f}}_{M^*}})$, and the added sparsity in the discipline couplings, that is measured by $\mathcal{P}(M^*)$.

With increasing values for λ, the objective in the optimization problem adds a greater penalty to models with less sparsity in the discipline couplings. This results in a set of increasingly sparser models that remove additional couplings at the expense of accuracy in the output distribution. These decoupled models for 4 different values of λ in $\Lambda = [10^{-4}, 10^{-3}, 10^{-1}, 10^{0}]$ are presented in Figures 7-14 with the decoupled connections indicated by dashed lines. The joint distribution for the output variables, $\pi_{\mathbf{f}_{M^*}}$, of the optimal model corresponding to each value of λ is also plotted in the figures below.

For the fire detection satellite model, the algorithm identifies that the feedback coupling variable between the Attitude Control and Power disciplines for the moment of inertia (I_{max}, and I_{min}) could be fixed to their mean value while having a small effect on the accuracy of joint output distribution, as seen in Figures 7 and 8. With increasing values for λ, the slewing angle, the satellite velocity, and the orbit period are also found to weakly contribute to the total torque and the overall power requirement for the attitude control subsystem, as seen in Figures 9 and 10. The subsequent sparser model for $\lambda = 10^{-1}$ fixes these discipline coupling variables along with the state inputs to the power discipline for the orbit and eclipse period. Finally, we note that for $\lambda = 10^{0}$, the optimal model has fully decoupled disciplines and the joint distribution for its output variables is given in Figure 14.

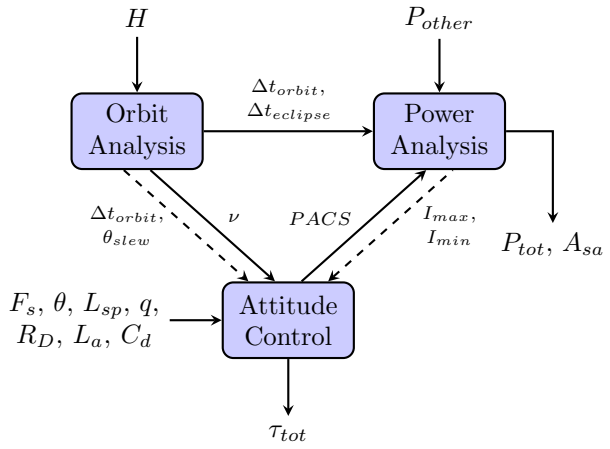

Figure 7. Optimal model coupling for $\lambda = 1.0 \times 10^{-4}$

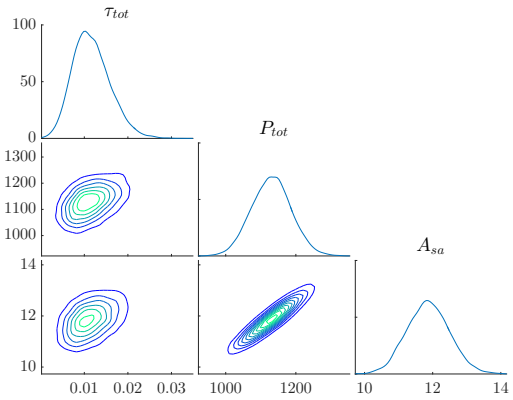

Figure 8. Joint distributions for $\lambda = 1.0 \times 10^{-4}$

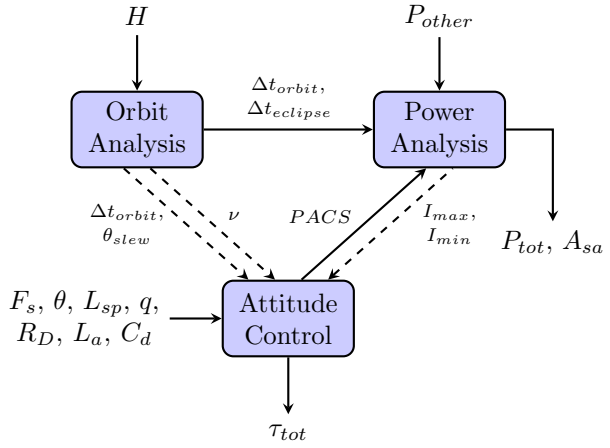

Figure 9. Optimal model coupling for $\lambda = 1.0 \times 10^{-3}$

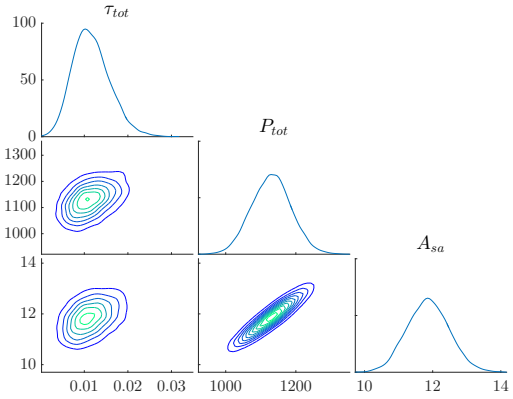

Figure 10. Joint distributions for $\lambda = 1.0 \times 10^{-3}$

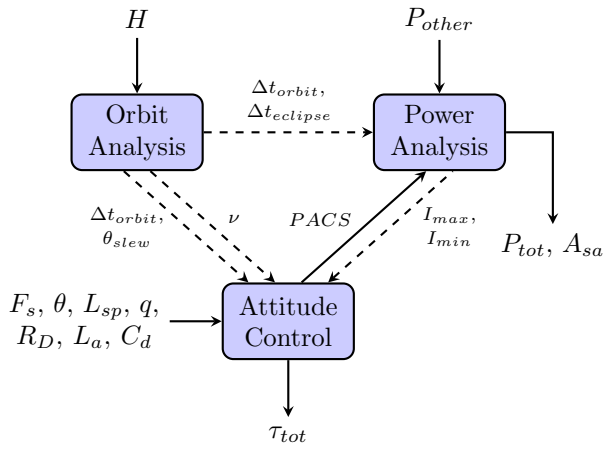

Figure 11. Optimal model coupling for $\lambda = 1.0 \times 10^{-1}$

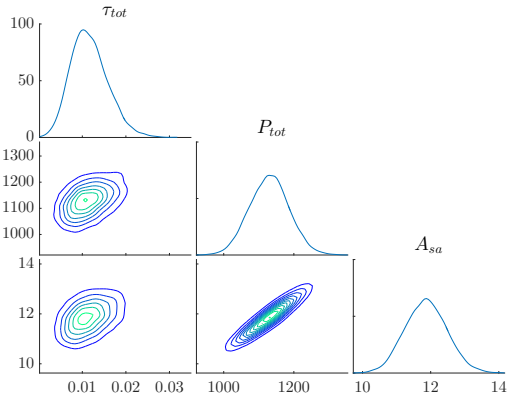

Figure 12. Joint distributions for $\lambda = 1.0 \times 10^{-1}$

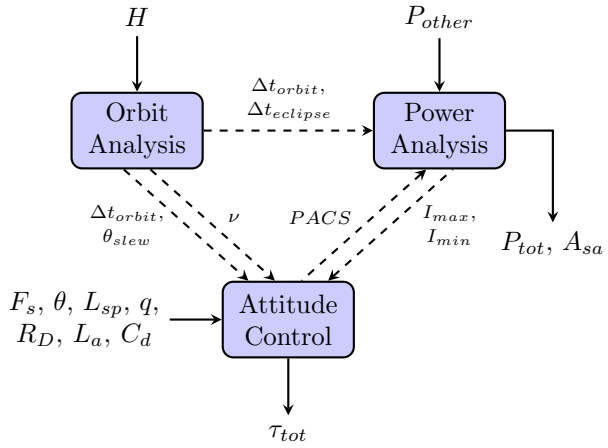

Figure 13. Optimal model coupling for $\lambda = 1.0 \times 10^{0}$

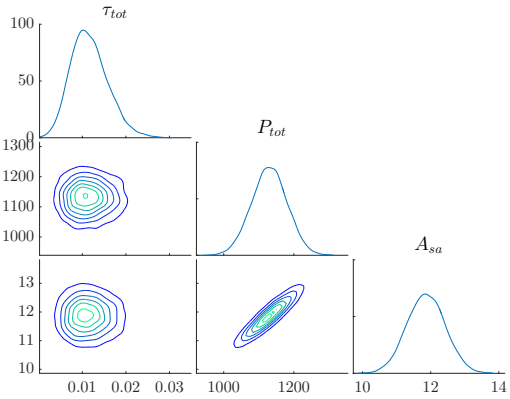

Figure 14. Joint distributions for $\lambda = 1.0 \times 10^{0}$

Furthermore, in Table 2 we present the values for the KL divergence between the Gaussian distribution for the linearized outputs of the reference model, M_0, and the optimally decoupled models, M^*, that we denote as linearized KL divergence. The number of active coupling variables, representing the increasing sparsity of each decoupled model with larger values of λ, is also presented in the table below.

Table 2. Linearized KL divergence for optimally decoupled models of the fire detection satellite

	$\lambda = 1 \times 10^{-4}$	$\lambda = 1 \times 10^{-3}$	$\lambda = 1 \times 10^{-1}$	$\lambda = 1 \times 10^{0}$
Linearized KL Divergence	7.30×10^{-16}	7.43×10^{-4}	4.20×10^{-3}	1.33×10^{-1}
Active Coupling Variables	4/8	3/8	1/8	0/8

From the table and figures above, we observe that the optimal models identified by the model selection algorithm corresponding to $\lambda \in [10^{-4}, 10^{-1}]$ result in very similar distributions for the model outputs as the reference model based on the linearized KL divergence. Furthermore, while the final optimal model for $\lambda = 10^0$ approximately captures the marginal uncertainty in the outputs, this fully decoupled model does not represent, as accurately, the correlations between the output variables, as seen in the joint marginal distribution of P_{tot} and τ_{tot} in Figure 14. Nevertheless, given that all decoupled models feature only feed-forward connections, these approximate coupling models can be used to cheaply propagate the uncertainty in the multidisciplinary model without having to iteratively solve for the outputs that correspond to each set of input variables. This results in a substantial computational savings for performing forward UQ. In particular,

if low accuracy is sufficient in the output uncertainty, the disciplines can be analyzed independently using the model corresponding to $\lambda = 10^0$.

Finally, we analyze the pointwise errors of the three model outputs in each decoupled model, M^*, relative to the reference model, M_0. The pointwise error is given by the difference in the values of the output variables in the decoupled and reference models for the same input sample. The errors for 10^4 input samples are displayed in Figures 15-18. With an increase in λ, the sparser models result in progressively greater pointwise errors, which are seen in the greater spread of the output values between both models. Although the set of discipline couplings corresponding to $\lambda = 10^{-1}$, and 10^0 have relatively accurate joint distributions for the model output uncertainty, their larger pointwise errors makes them less adequate for computations that require accurate pointwise approximations, such as multidisciplinary optimization. Nevertheless, the models associated with $\lambda = 10^{-4}$, and 10^{-3} (Figures 7 and 9) have accurate distributions for the output variables and low pointwise errors relative to the reference model, M_0.

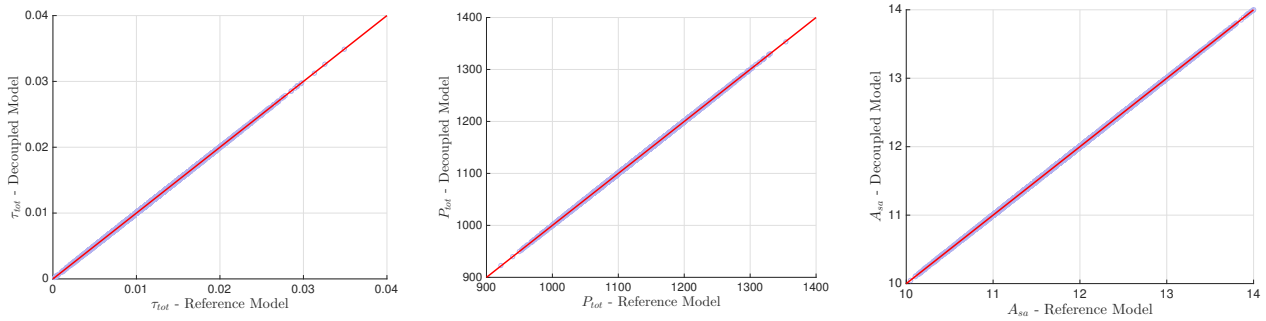

Figure 15. Comparison of QoI with optimally decoupled model for $\lambda = 1.0 \times 10^{-4}$

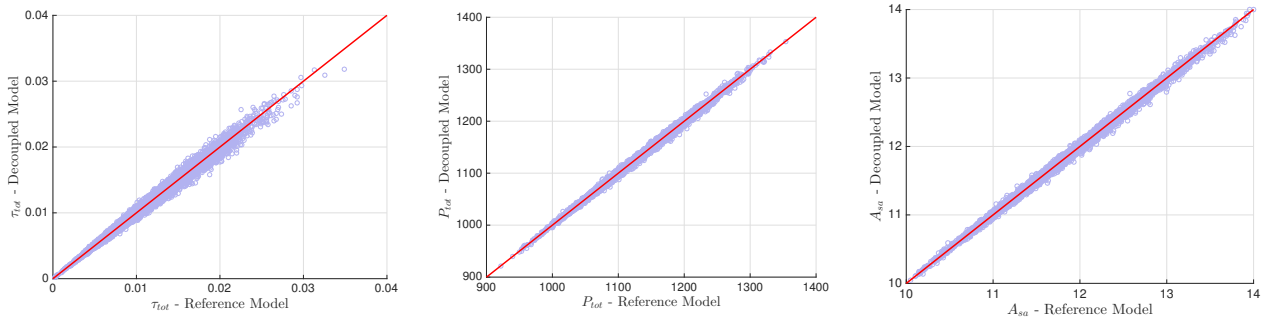

Figure 16. Comparison of QoI with optimally decoupled model for $\lambda = 1.0 \times 10^{-3}$

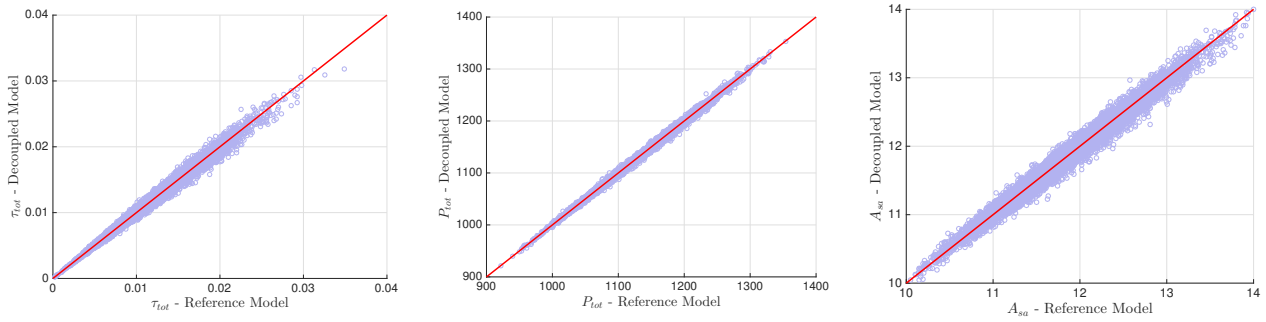

Figure 17. Comparison of QoI with optimally decoupled model for $\lambda = 1.0 \times 10^{-1}$

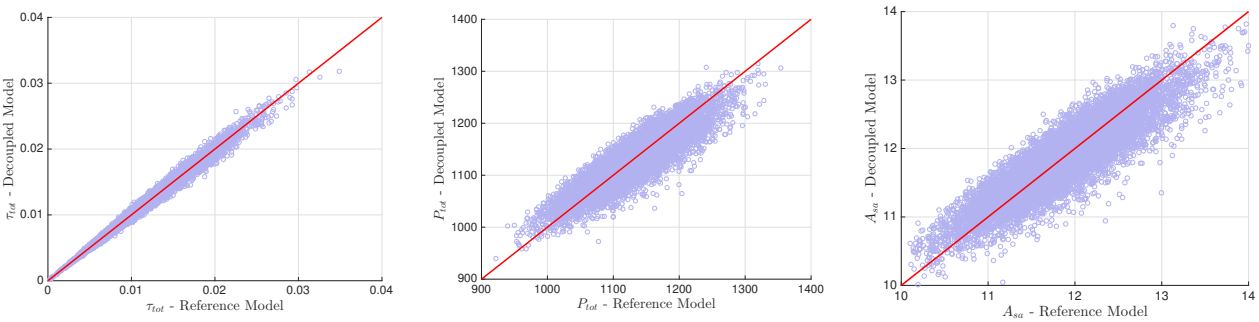

Figure 18. Comparison of QoI with optimally decoupled model for $\lambda = 1.0 \times 10^0$

IV.B. Turbine Engine Model

A model for turbine engine cycle analysis was first presented in Ref. 38. The reference model for the system, M_0, is displayed in Figure 19 and consists of 13 disciplines for the 12 engine components and a performance function, which are connected by 22 coupling variables. These disciplines model the engine with a core air-stream passing through a fan, compressor, burner and turbine as well as a second stream of air that bypasses the engine core. For each set of inputs that include the fan pressure ratio (FPR), compressor pressure ratio (CPR), bypass ratio (BPR), and mass-flow rate (W), the system's disciplines iteratively solve for 4 output quantities of interest: thrust-specific fuel consumption ($TSFC$), net thrust (F_n), overall pressure ratio (OPR), and engine burner temperature (T_4).

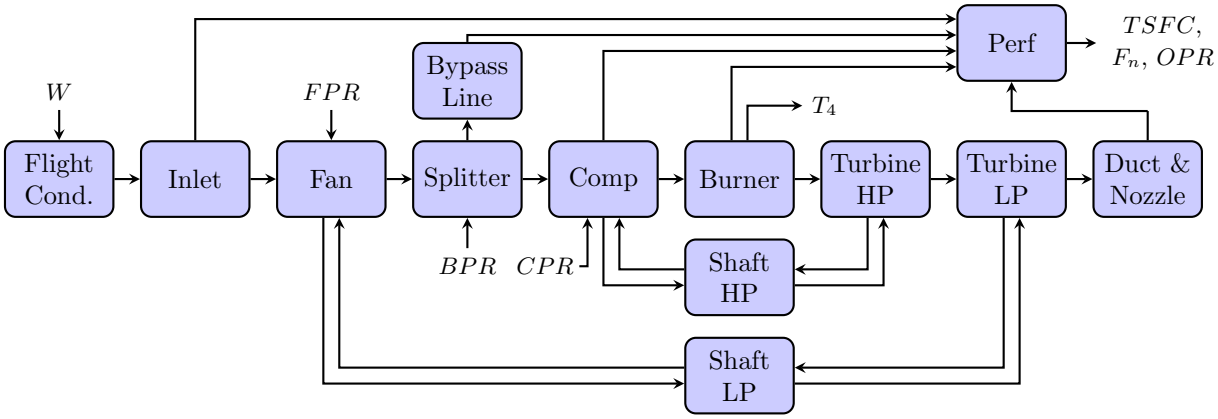

Figure 19. Turbine engine cycle model from Ref. 38

To analyze various operating conditions, the model inputs are represented with Gaussian distributed random variables whose parameters are listed in Table 3.

Table 3. Random variable parameters in the turbine engine cycle model

Random Variable	Symbol	Mean	Standard Deviation
Fan pressure ratio	FPR	1.5	0.01
Compressor pressure ratio	CPR	15.0	0.10
Bypass ratio	BPR	2.0	0.10
Mass-flow rate	W	1000.0	$\sqrt{10.0}$

By propagating 10^3 Monte Carlo samples of these inputs through the nonlinear system, the non-Gaussian distribution of the output variables is empirically characterized for the selected QoI in Figure 20. In the

optimal model selection algorithm, we use the linearizations of these output variables with respect to the inputs and compare the resulting multivariate Gaussian approximations to $\pi_{\mathbf{f}}$ with different subsets of the discipline couplings.

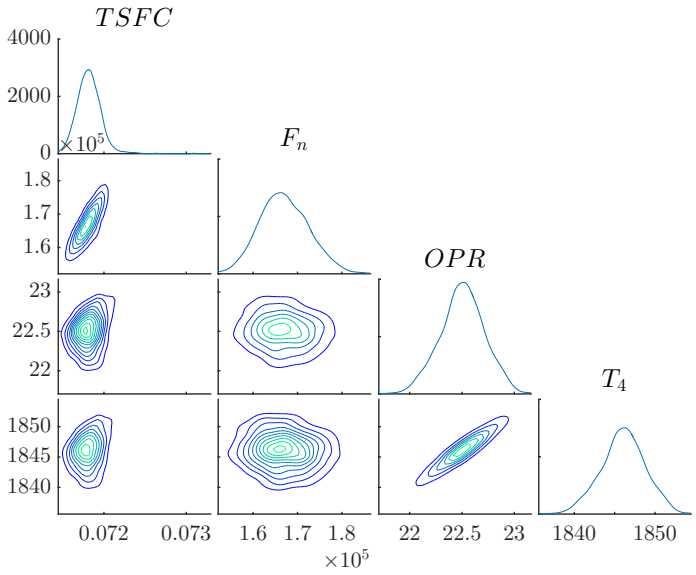

Figure 20. Joint distributions of the reference model

Applying the model selection procedure described above with $L = 1000$ particles, the SMC algorithm identifies decoupled models for four different values of λ in $\Lambda = [10^{-1}, 10^{0}, 10^{1}, 10^{3}]$. These models are presented in Figures 21-24 with the decoupled connections indicated by dashed lines. Similarly to the satellite model, we observe that with an increase in λ, the optimal solutions to the combinatorial optimization problem have greater sparsity in the number of discipline couplings. This results in a set of nested models that sequentially remove weak connections to increase the sparsity of couplings in exchange for accuracy in the output distributions. For this turbine engine case study with $\lambda = 10^{-1}$, and $\lambda = 10^{0}$, this results in neglecting the effect of the feedback from the low-pressure turbine on the fan and the variability of inlet ram drag on system performance.

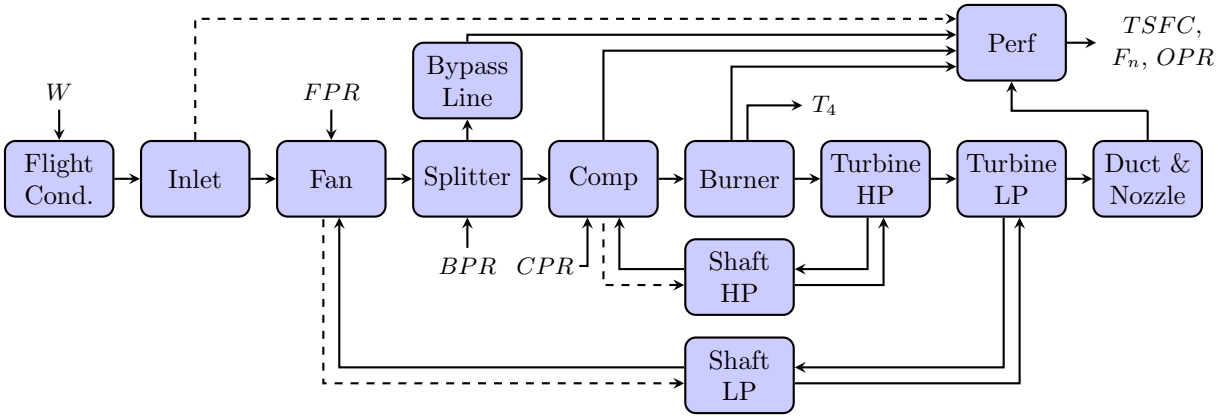

Figure 21. Optimal model coupling for $\lambda = 1.0 \times 10^{-1}$

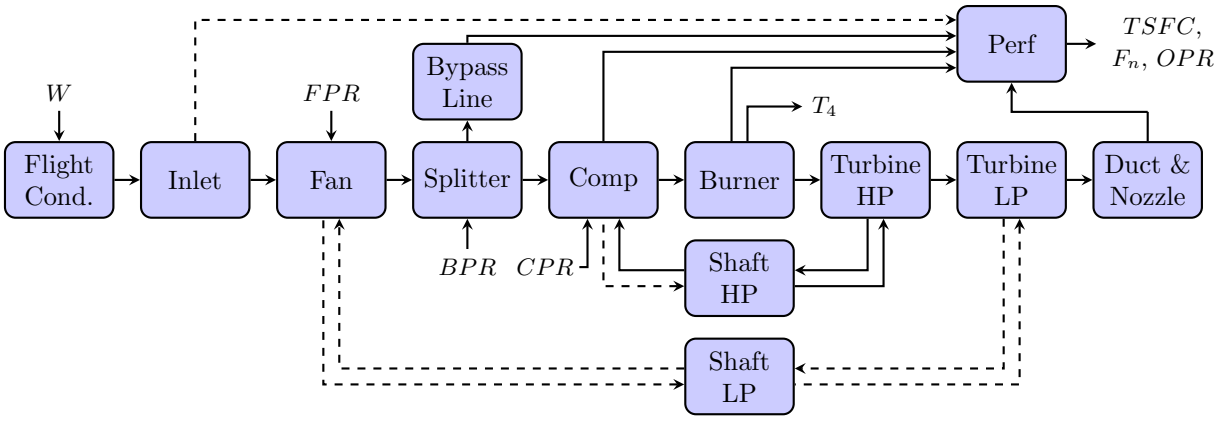

Figure 22. Optimal model coupling for $\lambda = 1.0 \times 10^0$

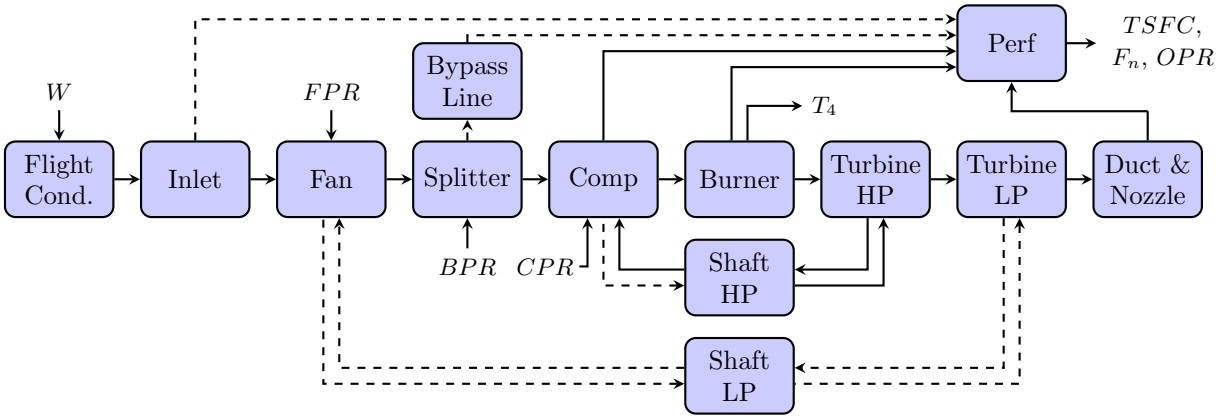

Figure 23. Optimal model coupling for $\lambda = 1.0 \times 10^1$

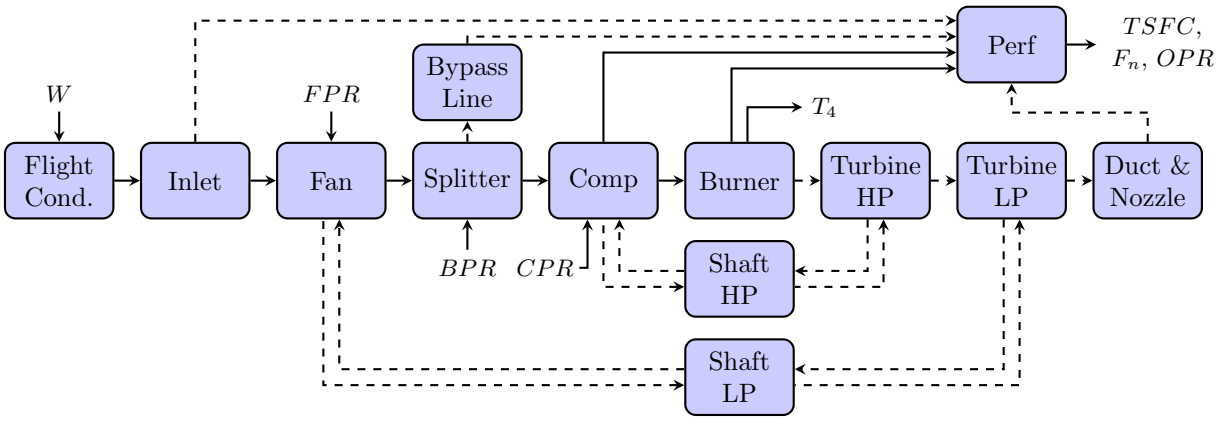

Figure 24. Optimal model coupling for $\lambda = 1.0 \times 10^3$

With a further increase in λ and a greater penalty on low sparsity models, the effect of the bypass line and the feedback from the high-pressure turbine are also neglected in the optimal models presented above. The accuracy of the system outputs corresponding to the decoupled model for each value of λ is displayed in the joint distributions of the output QoI in Figures 25-28. We observe that while the distribution for the output $TSFC$ variable is closely captured with the decoupled models for $\lambda = 10^{-1}$, and 10^0, the correlations of this variable are not as accurately represented when ignoring connections from the bypass line and feedback from the high-pressure turbine. This effect on the correlation is expected given the tight balance between the

bypass flow and the core flow through the high pressure turbine, that together produce most of the engine's thrust.

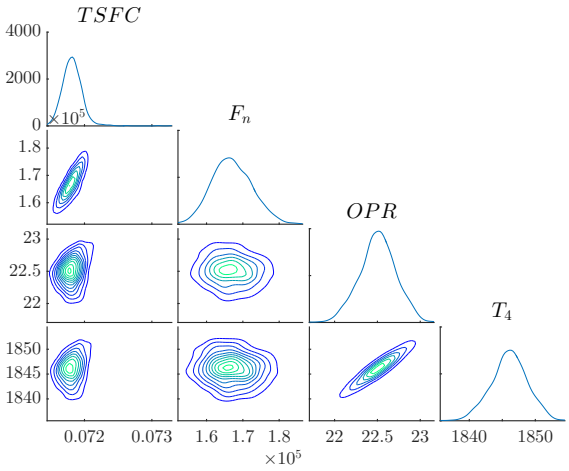

Figure 25. Joint distributions for $\lambda = 1.0 \times 10^{-1}$

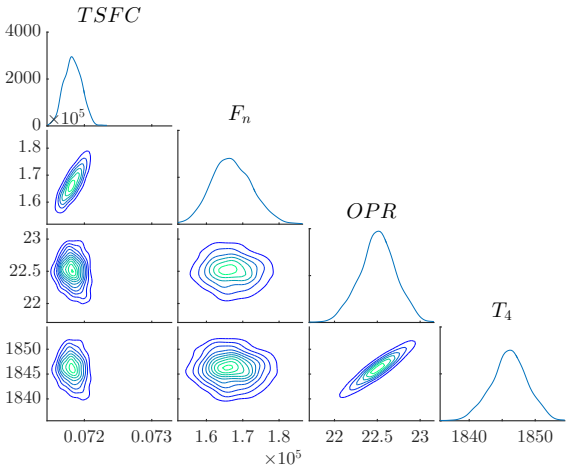

Figure 26. Joint distributions for $\lambda = 1.0 \times 10^{0}$

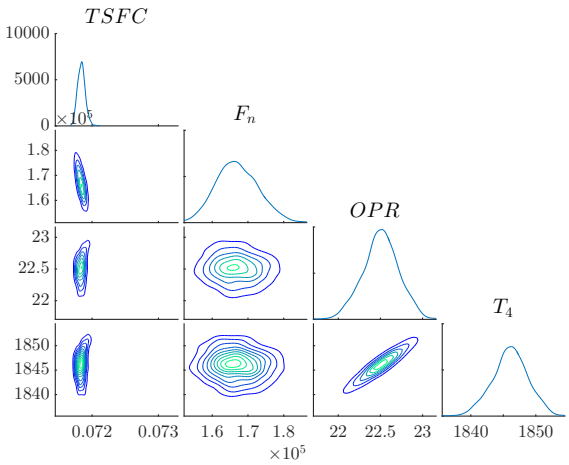

Figure 27. Joint distributions for $\lambda = 1.0 \times 10^{1}$

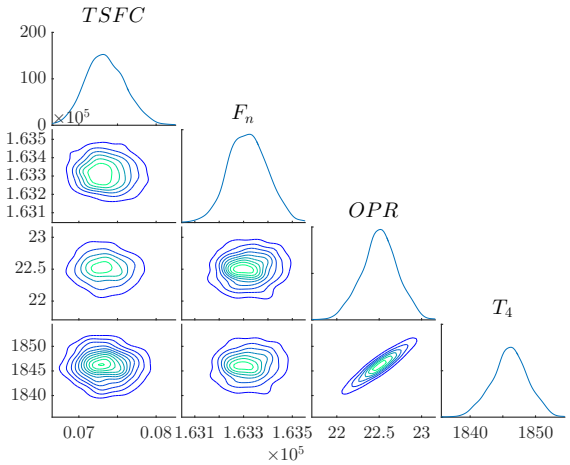

Figure 28. Joint distributions for $\lambda = 1.0 \times 10^{3}$

Furthermore, while the first three models accurately capture the net thrust, F_n, the uncertainty in this variable is poorly represented with the last model when ignoring the contribution of the nozzle. Finally, all four models accurately represent the uncertainty in the overall pressure ratio, OPR, and engine burner temperature, T_4. As a result, depending on the application and available computational resources, users may select the appropriate set of discipline couplings for the turbine engine to model the system uncertainty in the output variables.

To quantitatively compare the decoupled models, we also present the linearized KL divergence between the approximating Gaussian distributions for the reference and optimally decoupled models of the turbine engine in Table 4. These results are presented along with the number of active coupling variables in each model (i.e., solid lines in the model diagrams above) that demonstrates the increasing sparsity in the decoupled models for larger values of λ.

Table 4. Linearized KL divergence for optimally decoupled models of the turbine engine

	$\lambda = 1 \times 10^{-1}$	$\lambda = 1 \times 10^{0}$	$\lambda = 1 \times 10^{1}$	$\lambda = 1 \times 10^{3}$
Linearized KL Divergence	6.95×10^{-10}	1.15×10^{0}	1.25×10^{1}	3.73×10^{3}
Active Coupling Variables	19/22	16/22	14/22	7/22

To further compare the models, the pointwise errors of the three outputs from the performance discipline ($TSFC$, F_n, and OPR) for the decoupled models corresponding to $\lambda = 10^{-1}$, 10^0, and 10^1 are plotted in Figures 29-31. These figures demonstrate the increasing errors in the outputs of the decoupled models relative to the reference model at the same inputs for 10^3 samples with the reduction in the number of discipline couplings. With the exception of the $TSFC$ output variable in the final model (Figure 31), the trends for the output variables are closely captured by the decoupled models associated with $\lambda = 10^{-1}$, and 10^0. Nevertheless, users with different requirements may still trade-off sparsity and accuracy for performing computations, such as multidisciplinary optimization, with these two decoupled models. While the optimal model for $\lambda = 10^0$ eliminates one feedback cycle from the low pressure turbine leading to lower computational costs than the model for $\lambda = 10^{-1}$, there is a trade-off with accuracy, as seen with the larger spread in the pointwise errors of the $TSFC$ variable.

Furthermore, this result highlights the importance of the bypass line to accurately estimate $TSFC$ when computing the turbine's performance. We note that this coupling is included in the models corresponding to $\lambda = 10^{-1}$, and 10^0.

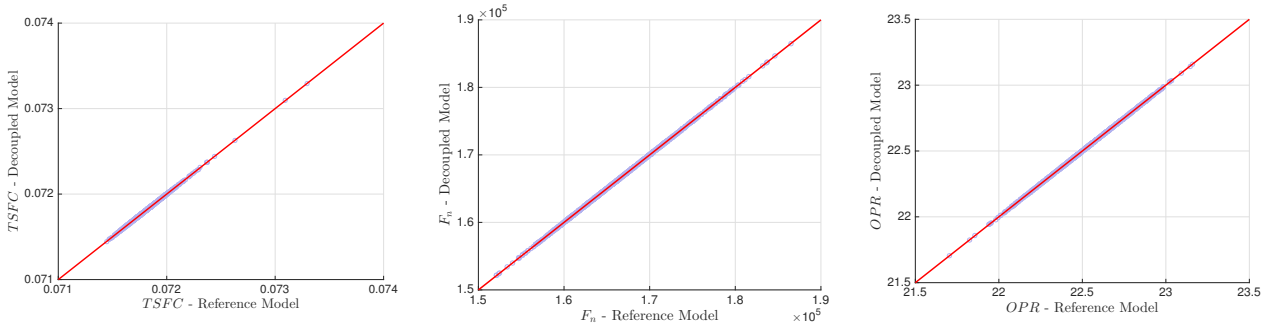

Figure 29. Comparison of QoI with optimally decoupled model for $\lambda = 1.0 \times 10^{-1}$

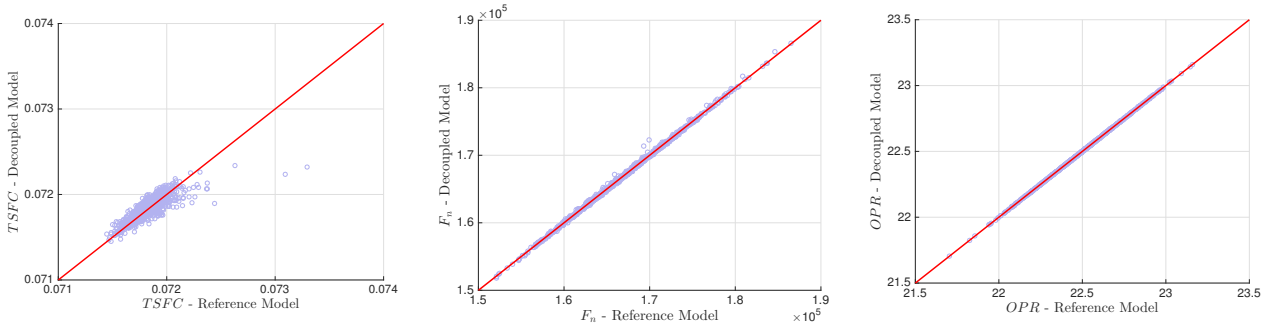

Figure 30. Comparison of QoI with optimally decoupled model for $\lambda = 1.0 \times 10^{0}$

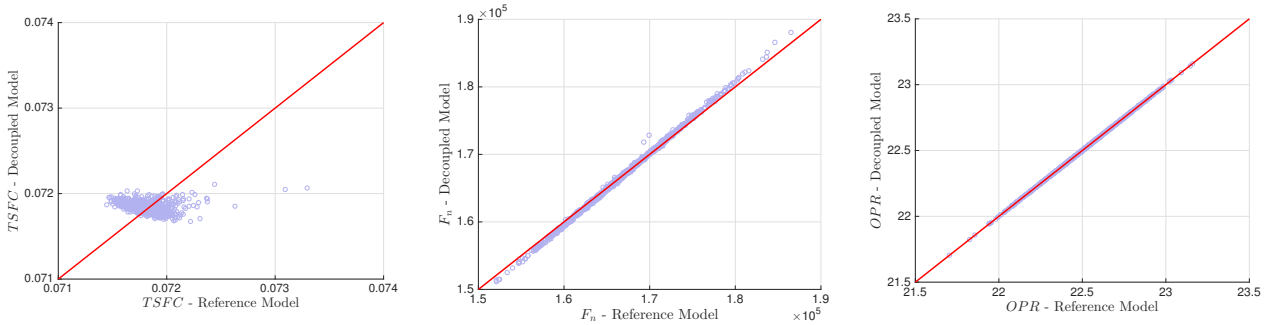

Figure 31. Comparison of QoI with optimally decoupled model for $\lambda = 1.0 \times 10^{1}$

Finally, in addition to producing a sequence of sparsely coupled models with a reduced number of discipline couplings relative to M_0, the model selection algorithm efficiently found all of the optimally decoupled models by visiting less than 5.7% of the model space. This is contrasted with the otherwise intractable process of enumerating all possible models to find the optimum of the combinatorial problem posed in equation 3.

IV.C. Numerical Implementation

A publicly available MATLAB implementation of the algorithm to find the optimal approximate coupling for a multidisciplinary model can be found at `www.github.com/baptistar/coupling`. The application of the algorithm to the fire detection satellite model presented in this work is publicly available for reference.

V. Conclusion

Identifying important discipline couplings in the context of multidisciplinary models under uncertainty has been studied from the perspective of optimal model selection. Using a combination of model linearizations and sequential Monte Carlo, the combinatorial model space was efficiently explored for two engineering problems: a fire detection satellite model and a turbine engine cycle analysis model. This resulted in a set of optimal models with a reduced number of discipline couplings relative to the reference model, while remaining accurate in distribution for the specified output quantities of interest.

Future research will address corrections to the Gaussian approximations used in the algorithm by using a small number of samples from the reference model to improve the estimates for the KL divergence. Furthermore, the selection of other informative functions for $\mathcal{P}(M)$ to model the complexity of each model will be considered by taking into account the computational cost of keeping each discipline coupling. Finally, the continued application of the algorithm to reveal the natural structure of other complex engineering systems under different input uncertainties will also be explored.

VI. Acknowledgment

This work has been supported in part by the Air Force Office of Scientific Research (AFOSR) MURI on "Managing multiple information sources of multi-physics systems," Program Officer Jean-Luc Cambier, Award Number FA9550-15-1-0038. The authors also thank T. Hearn and J. Gray for supplying the turbine engine cycle model.

References

[1]Cramer, E. J., Dennis, Jr, J., Frank, P. D., Lewis, R. M., and Shubin, G. R., "Problem formulation for multidisciplinary optimization," *SIAM Journal on Optimization*, Vol. 4, No. 4, 1994, pp. 754–776.

[2]Martins, J. R. R. A. and Hwang, J. T., "Review and unification of methods for computing derivatives of multidisciplinary computational models," *AIAA journal*, Vol. 51, No. 11, 2013, pp. 2582–2599.

[3]Gage, R. B. P. and lan Sobieski, I. K., "Implementation and performance issues in collaborative optimization," *AIAA Paper*, 1996.

[4]Bloebaum, C. L., Hajela, P., and Sobieszczanski-Sobieski, J., "Non-hierarchic system decomposition in structural optimization," *Engineering Optimization+ A35*, Vol. 19, No. 3, 1992, pp. 171–186.

[5]Sellar, R., Batill, S., and Renaud, J., "Response surface based, concurrent subspace optimization for multidisciplinary system design," *AIAA paper*, Vol. 714, 1996, pp. 1996.

[6]Sobieszczanski-Sobieski, J., Agte, J. S., and Sandusky, R. R., "Bilevel integrated system synthesis," *AIAA journal*, Vol. 38, No. 1, 2000, pp. 164–172.

[7]Kim, H. M., Michelena, N. F., Papalambros, P. Y., and Jiang, T., "Target cascading in optimal system design," *Journal of mechanical design*, Vol. 125, No. 3, 2003, pp. 474–480.

[8]Haftka, R. T., "Optimization of flexible wing structures subject to strength and induced drag constraints," *AIAA Journal*, Vol. 15, No. 8, 1977, pp. 1101–1106.

[9]Sobieszczanski-Sobieski, J. and Haftka, R. T., "Multidisciplinary aerospace design optimization: survey of recent developments," *Structural optimization*, Vol. 14, No. 1, 1997, pp. 1–23.

[10]Kroo, I., Altus, S., Braun, R., Gage, P., and Sobieski, I., "Multidisciplinary optimization methods for aircraft preliminary design," *AIAA paper*, Vol. 4325, 1994, pp. 1994.

[11]Martins, J. R. R. A., Alonso, J. J., and Reuther, J. J., "High-fidelity aerostructural design optimization of a supersonic business jet," *Journal of Aircraft*, Vol. 41, No. 3, 2004, pp. 523–530.

[12]McAllister, C. D. and Simpson, T. W., "Multidisciplinary robust design optimization of an internal combustion engine," *Journal of mechanical design*, Vol. 125, No. 1, 2003, pp. 124–130.

[13]Fuglsang, P. and Madsen, H. A., "Optimization method for wind turbine rotors," *Journal of Wind Engineering and Industrial Aerodynamics*, Vol. 80, No. 1, 1999, pp. 191–206.

[14]Braun, R. D., Moore, A. A., and Kroo, I. M., "Collaborative approach to launch vehicle design," *Journal of spacecraft and rockets*, Vol. 34, No. 4, 1997, pp. 478–486.

[15]Keyes, D., "Computational Science," *The Princeton Companion to Applied Mathematics*, Princeton University Press, 2015.

[16]Steward, D. V., "The design structure system: A method for managing the design of complex systems," *IEEE transactions on Engineering Management*, , No. 3, 1981, pp. 71–74.

[17]Lu, Z. and Martins, J., "Graph partitioning-based coordination methods for large-scale multidisciplinary design optimization problems," *12th AIAA Aviation Technology*, 2012.

[18]Schäfer, C. and Chopin, N., "Sequential Monte Carlo on large binary sampling spaces," *Statistics and Computing*, Vol. 23, No. 2, 2013, pp. 163–184.

[19]Zhou, Y., Johansen, A. M., and Aston, J. A., "Towards automatic model comparison: an adaptive sequential Monte Carlo approach," *Journal of Computational and Graphical Statistics*, 2015.

[20]Brevault, L., Balesdent, M., Bérend, N., and Le Riche, R., "Decoupled multidisciplinary design optimization formulation for interdisciplinary coupling satisfaction under uncertainty," *AIAA Journal*, Vol. 54, No. 1, 2015, pp. 186–205.

[21]Smith, R. C., *Uncertainty quantification: theory, implementation, and applications*, Vol. 12, SIAM, 2013.

[22]Amaral, S., Allaire, D., and Willcox, K., "A decomposition-based approach to uncertainty analysis of feed-forward multicomponent systems," *International Journal for Numerical Methods in Engineering*, Vol. 100, No. 13, 2014, pp. 982–1005.

[23]Sankararaman, S. and Mahadevan, S., "Likelihood-based approach to multidisciplinary analysis under uncertainty," *Journal of Mechanical Design*, Vol. 134, No. 3, 2012, pp. 031008.

[24]Arnst, M., Ghanem, R., Phipps, E., and Red-Horse, J., "Dimension reduction in stochastic modeling of coupled problems," *International Journal for Numerical Methods in Engineering*, Vol. 92, No. 11, 2012, pp. 940–968.

[25]Arnst, M., Soize, C., and Ghanem, R., "Hybrid sampling/spectral method for solving stochastic coupled problems," *SIAM/ASA Journal on Uncertainty Quantification*, Vol. 1, No. 1, 2013, pp. 218–243.

[26]Arnst, M., Ghanem, R., Phipps, E., and Red-Horse, J., "Reduced chaos expansions with random coefficientsin reduced-dimensional stochastic modeling of coupled problems," *International Journal for Numerical Methods in Engineering*, Vol. 97, No. 5, 2014, pp. 352–376.

[27]Jin, R., Chen, W., and Simpson, T., "Comparative studies of metamodelling techniques under multiple modelling criteria," *Structural and Multidisciplinary Optimization*, Vol. 23, No. 1, 2001, pp. 1–13.

[28]Chaudhuri, A. and Willcox, K., "Multifidelity Uncertainty Propagation in Coupled Multidisciplinary Systems," *18th AIAA Non-Deterministic Approaches Conference*, 2016, p. 1442.

[29]MacKay, D. J., *Information theory, inference and learning algorithms*, Cambridge university press, 2003.

[30]Seshadri, P., Constantine, P., Iaccarino, G., and Parks, G., "A density-matching approach for optimization under uncertainty," *Computer Methods in Applied Mechanics and Engineering*, Vol. 305, 2016, pp. 562–578.

[31]Mahadevan, S. and Haldar, A., "Probability, reliability and statistical method in engineering design," 2000.

[32]Jameson, A., "Aerodynamic design via control theory," *Journal of scientific computing*, Vol. 3, No. 3, 1988, pp. 233–260.

[33]Martins, J. R. R. A., Alonso, J. J., and Reuther, J. J., "A coupled-adjoint sensitivity analysis method for high-fidelity aero-structural design," *Optimization and Engineering*, Vol. 6, No. 1, 2005, pp. 33–62.

[34]Proctor, W. C., *Elements of high-order predictive model calibration algorithms with applications to large-scale reactor physics systems*, North Carolina State University, 2012.

[35]Ausiello, G., Crescenzi, P., Gambosi, G., Kann, V., Marchetti-Spaccamela, A., and Protasi, M., *Complexity and Approximation: Combinatorial Optimization Problems and Their Approximability Properties*, Springer Berlin Heidelberg, 2012.

[36]Del Moral, P., Doucet, A., and Jasra, A., "Sequential Monte Carlo samplers," *Journal of the Royal Statistical Society: Series B (Statistical Methodology)*, Vol. 68, No. 3, 2006, pp. 411–436.

[37]Schäfer, C., "Particle algorithms for optimization on binary spaces," *ACM Transactions on Modeling and Computer Simulation (TOMACS)*, Vol. 23, No. 1, 2013, pp. 8.

[38]Hearn, T., Hendricks, E., Chin, J., Gray, J., and Moore, K. T., "Optimization of Turbine Engine Cycle Analysis with Analytic Derivatives," *17th AIAA/ISSMO Multidisciplinary Analysis and Optimization Conference*, 2016, p. 4297.